GEOLOGICA CARPATHICA, AUGUST 2017, 68, 4, 366–381 doi: 10.1515/geoca-2017-0025

Bi-sulphotellurides associated with Pb–Bi–(Sb±Ag,Cu,Fe) sulphosalts: an example from the Stan Terg deposit in Kosovo

JOANNA KOŁODZIEJCZYK[1]✉, JAROSLAV PRŠEK[1], PANAGIOTIS CH. VOUDOURIS[2] and VASILIOS MELFOS[3]

[1]AGH University of Science and Technology, Faculty of Geology, Geophysics and Environmental Protection, Department of Economic Geology, al. Mickiewicza 30, 30-059 Kraków, Poland; ✉asia.office@wp.pl (J.K.), prsek@geol.agh.edu.pl (J.P.)
[2]Department of Mineralogy-Petrology, National and Kapodistrian University of Athens, Athens 15784, Greece; voudouris@geol.uoa.gr
[3]Department of Mineralogy, Petrology and Economic Geology, Aristotle University of Thessaloniki, Thessaloniki 54124, Greece; melfosv@geo.auth.gr

(Manuscript received December 26, 2016; accepted in revised form March 15, 2017)

Abstract: New mineralogical and mineral-chemical data from the Stan Terg deposit, Kosovo, revealed the presence of abundant Bi-sulphotellurides associated with Bi- and Sb-sulphosalts and galena in pyrite–pyrrhotite-rich skarn-free ore bodies (ores without skarn minerals). The Bi-bearing association comprises Bi-sulphotellurides (joséite-A, joséite-B, unnamed phase A with a chemical formula close to $(Bi,Pb)_2(TeS)_2$, unnamed phase B with a chemical composition close to $(Bi,Pb)_{2.5}Te_{1.5}S_{1.5}$), ikunolite, cosalite, Sb-lillianite, members of the kobellite series and Bi-jamesonite. Compositional trends of the Bi-sulphotellurides suggest lattice-scale incorporation of Bi–(Pb)-rich module and/or admixture with submicroscopic PbS layers in modulated structures, or complicated Bi–Te substitution. Cosalite is characterized by high Sb (max. 3.94 apfu), and low Cu and Ag (up to 0.72 apfu of Cu+Ag). Jamesonite from this mineralization has elevated Bi content, from 0.85 to 2.30 apfu. The negligible content of Au and Ag in the Bi-sulphotellurides, the low content of Ag in Bi-sulphosalts, together with the lack of Au–Ag bearing phases in the mineralization, indicate either ore deposition from fluid(s) depleted in precious metals, or physico-chemical conditions of ore formation preventing Au and Ag precipitation at the deposit site. The temperature of initial mineralization may have exceeded 400 ºC as suggested by the lamellar exsolution textures observed in lillianite, which indicate breakdown textures from decomposition of high-temperature initial crystals. Non-stoichiometric phases among the Bi-sulphosalts and sulphotellurides studied at Stan Terg reflect modulated growth processes in a metasomatic environment.

Keywords: Kosovo, Stan Terg, Bi-tellurides, tetradymite group minerals, Sb-cosalite, Sb-lillianite, kobellite homologous series.

Introduction

Bismuth sulphotellurides are common mineral phases occurring in high-temperature associations with Bi-sulphosalts and Au mineralization in Pb–Zn skarn deposits (Cook et al. 2007a), VHMS deposits (Vikentyev 2006), orogenic Au deposits (Bowell et al. 1990; Ciobanu et al. 2010), Au-bearing quartz-veins in intrusion-related systems (Cepedal et al. 2013), nickel mineralization in greenstone belts (Groves & Hall 1978), and porphyry-epithermal systems (Cook & Ciobanu 2004; Melnikov et al. 2009; Pršek & Peterec 2008; Plotinskaya et al. 2009). Tellurium mineralization, together with Bi, is commonly linked to Au occurrences (Ciobanu et al. 2009a; Cook et al. 2009).

Bismuth sulphotellurides are stable over a wide temperature interval and their composition reflects the geochemical characteristics of the mineralization environment (Melnikov et al. 2009).

The tetradymite group comprises 19 mineral species and several unknown phases which can be ordered into the following subspecies: Bi_2Te_3–Bi_2Se_3–Bi_2S_3, Bi_4Te_3–Bi_4Se_3–Bi_4S_3 and BiTe–BiSe–BiS (Cook et al. 2007a). These minerals have usually rhombohedral- or trigonal-layered structures and limited variation in composition. Minor Pb↔Bi substitution is widespread throughout the group, especially in the Bi_4Te_3–Bi_4Se_3–Bi_4S_3 subgroup.

The precise identification of sulphotelluride phases is not easy because they are commonly intergrown with each other on the submicroscopic scale. Due to the small size of mineral aggregates, X-ray diffraction structural data cannot be obtained, hence many unknown sulphotelluride phases identified by EPMA, could not be thoroughly characterized.

At the Stan Terg Pb–Zn(–Ag–Bi) deposit, within the Trepça Mineral Belt, in Kosovo, the Bi-bearing sulphosalts and chalcogenides, ikunolite, babkinite, joséite-A, izoklakeite, cannizzarite, lillianite-gustavite and heyrovskýite, were previously described in samples from galena-rich skarn mineralization (e.g., orebodies No. 140 and 149), and from arsenopyrite-rich skarn-free mineralization (corridor walls in the southern part of the Xth horizon) (Kołodziejczyk et al. 2015). Kołodziejczyk et al. (2015) suggested that the bismuth-bearing phases at Stan Terg were formed during the retrograde evolution of the hydrothermal system under generally low-sulphidation and reduced fluid states in the temperature range from 350 to 250 °C.

This study provides detailed mineralogical and geochemical data concerning new sulphotellurides found in association with Bi-sulphosalts in the Stan Terg deposit. Electron microprobe data are provided for all phases identified, and their physico-chemical conditions of formation are discussed in comparison with similar assemblages elsewhere.

Geological setting

Stan Terg, the largest known Pb–Zn deposit in Kosovo, hosts polymetallic mineralization with abundant assemblages containing Bi-, Sb-, Ag- and Sn-bearing minerals, and average ore grades at 3.65 % Pb, 3.55% Zn, and Bi, Ag and Sn as significant by-products (average 87 g/t Ag, 100 g/t Bi, and 30 g/t Sn).

The mineralization is related to the Tertiary (Oligocene–Miocene) magmatic activity that took place within the Trepça Mineral Belt, which is a part of the Vardar suture zone, stretching from the north to the south through the Balkan Peninsula, in southeastern Europe (Hyseni et al. 2010; Strmić Palinkaš et al. 2013). The significance of the Trepça Mineral belt has been confirmed by many authors who have described different types of Pb–Zn mineralization such as skarn, hydrothermal replacement, and vein mineralization considered to be controlled primarily by faults (e.g., Janković 1995).

The area around the Stan Terg deposit is composed of Triassic sedimentary and volcanoclastic rocks, upper Triassic carbonates, ophiolite mélange with Jurassic ultrabasic rocks and serpentinites, and Cretaceous series of clastics, serpentinites, volcanics and volcanoclastic rocks of basaltic composition and carbonates (Fig. 1A). The area is covered by Tertiary volcanics, like lavas, sub-volcanic intrusives and pyroclastic rocks, dominated by andesite, trachyte and latite composition (Hyseni et al. 2010). The mineralization in the Stan Terg deposit is related to post-collisional magmatism (Féraud & Deschamps 2009; Strmić Palinkaš et al. 2013), and the nearest magmatic rocks of calc-alkaline composition that are exposed on the surface are in the Kopaonik Massif, in the northern part of Kosovo.

Ore mineralization

The ore mineralization is hosted mostly within Triassic carbonates (marbles) in several elongated orebodies (eleven main orebodies) that plunge parallel and commonly join or split forming a type of large stockwork. The shape of orebodies is controlled by an anticline structure with carbonates in the core and shielded by sericite schists in the external part. The hydrothermal fluid transport was controlled by faults, fissures and palaeo-karst cavities. Until today, ore was excavated from 11 mining horizons, but the final depth has not been documented (Féraud & Deschamps 2009). There is also a volcanic conduit with phreatomagmatic breccias in the central part of the deposit (Féraud & Deschamps 2009; Strmić Palinkaš et al. 2013) that stretch parallel to the orebodies. Parts of the orebodies are related to skarn mineralization, parts are skarn-free carbonate-replacements (e.g., mantos-type), and significant ore precipitated as karst fillings. Karst fillings originated by the corrosive action of the metalliferous hydrothermal solutions dissolving the limestones (Forgan 1950; Schumacher 1950; Féraud et al. 2007).

The ore mineralization is dominated by galena, sphalerite, pyrite, pyrrhotite, arsenopyrite, with minor chalcopyrite, tetrahedrite, Sn-minerals, Bi-minerals, Ag-minerals and native elements (Kołodziejczyk et al. 2015, 2016a,b). The skarn alteration (garnet, hedenbergite, ilvaite and actinolite, magnetite) is present near the central volcanic conduit, but also in the distal parts of the deposit (Dangić 1993). The previously described Bi-sulphosalt mineralization is hosted in both skarn- and skarn-free orebodies and is considered to represent a single stage of mineral precipitation (Kołodziejczyk et al. 2015). The skarn orebodies usually contain a silicate paragenesis with base metal sulphides and Bi-minerals, whereas skarn-free orebodies with Bi-mineralization occur in the form of brecciated veins. Both mineralization types occur at the same depth level, close to the central breccia-pipe. Strmić Palinkaš et al. (2013) recognized a prograde magmatic stage (with precipitation of pyroxene and garnet), and following retrograde skarn and a hydrothermal stage dominated by ilvaite, magnetite, Pb-, Zn- and Fe-sulphides, quartz and carbonates. According to their work, the source of hydrothermal fluids is magmatic, and the fluid was partially mixed with meteoric waters during infiltration in the country rocks.

Sampling and methodology

The studied Bi–Pb–Sb–S–Te-bearing mineral assemblages were found in ten samples from recently developed orebodies; No. 141 and 140 in the Xth horizon of the Stan Terg mine (Fig. 1B).

The chemical composition of the sulphotellurides and sulphosalts were determined using a JEOL JXA-8230 Superprobe electron probe microanalyser (EPMA) in the Critical Elements Laboratory at the Faculty of Geology, Geophysics, and Environmental Protection, AGH University of Science and Technology in Krakow. All measurements were done on carbon-coated polished sections using the following operating conditions: accelerating voltage 20 kV, beam current 20 nA, and a beam diameter ~1 μm. The following spectral lines, standards (metals and sulphides), count times (peak and background for unknowns) were used: S (SK_α, FeS_2, 20 s, 10 s), Fe (FeK_α, FeS_2, 20 s, 10 s), Cu (CuK_α, Cu, 20 s, 10 s), Se (SeL_α, Se, 20 s, 10 s), Ag (AgL_α, Ag, 20 s, 10 s), Sb (SbL_α, Sb_2S_3, 20 s, 10 s), Te (TeL_α, PbTe, 20 s, 10 s), Pb (PbM_α, PbS, 20 s, 10 s), Mn (MnK_α, MnS, 20 s, 10 s) and Bi (BiM_α, Bi, 20 s, 10 s). The typical minimum detection limits for those analytical conditions were: Te (120 ppm), S (30 ppm), Pb (160 ppm), Bi (140 ppm), Cu (50 ppm), Fe (40 ppm), Ag (40 ppm), Sb (40 ppm), Se (80 ppm), Mn (120 ppm). Back-scattered

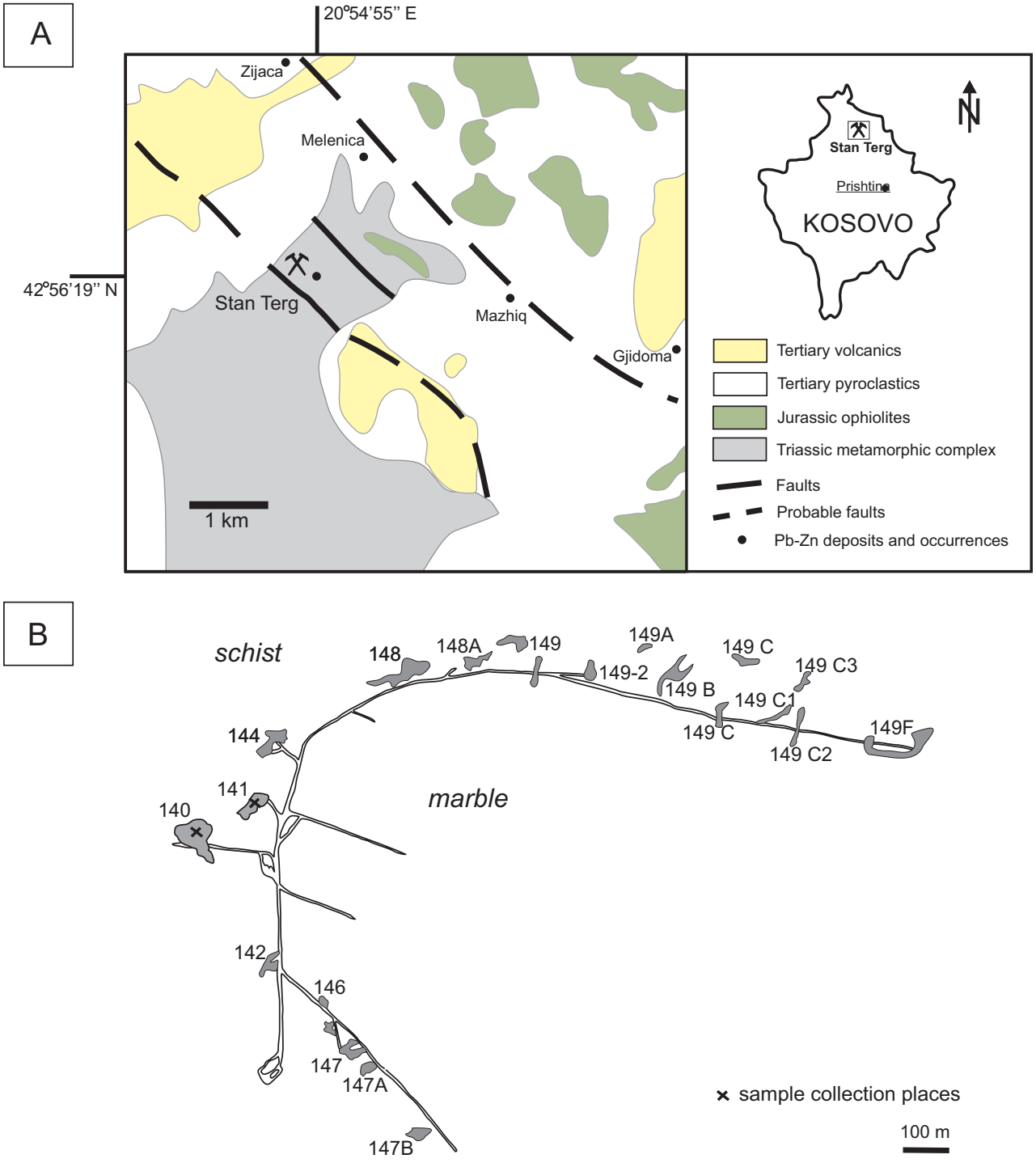

Fig. 1. A — Simplified geological map of the Trepça Mineral Belt with marked mines and occurrences of Pb–Zn mineralization (modified after Hyseni et al. 2010 and Kołodziejczyk et al. 2015). **B** — Simplified sketch of Xth mining horizon in the Stan Terg mine with orebodies and sample collection places.

electron (BSE) images provided information about internal structures (e.g., growth zoning, intergrowths, and replacement of analysed phases). X-ray maps were collected for selected intergrowths of telluride with Bi-sulphosalts and galena and the following elements were recorded: Ag*Lα*, Bi*Mα*, Sb*Lα*, Cu*Kα*, Fe*Kα*, Pb*Mα*, S*Kα*, Te*Lα*.

Results

Textures and petrography of the Te–Bi-mineral association

The newly discovered Bi–Sb–Pb–Te–S composite aggregates consist of sulphotellurides intergrown with Bi- and Sb-enriched

sulphosalts and with minor galena. This mineral association is dispersed between pyrite, marcasite, and pyrrhotite crystals hosted in a carbonate matrix (Fig. 2). Aggregates occur up to 500 μm in size, and single phases of sulphosalts recognized in BSE images are usually around 10–20 μm, whereas sulphotellurides are mostly up to 5 μm. The Bi-bearing association studied comprises Bi-sulphotellurides (joséite-A, joséite-B, unnamed phase A, unnamed phase B), ikunolite, cosalite, Sb-lillianite, kobellite series members and Bi-jamesonite.

Tellurides occur as elongated inclusions in cosalite or lillianite aggregates, with sizes up to 20 μm (Fig. 3A). In part of the inclusions, intergrowths composed of different chemical compositions are present, for example, phase A and phase B (Fig. 3B), or joséite-A and joséite-B (Fig. 3C,D). Phase A and phase B often form intergrowths with different Te concentrations in various parts of the cosalite crystals. Joséite-A and joséite-B occur primarily as intergrowths with native bismuth (Fig. 3D), or with ikunolite (Fig. 3E,F). Lillianite occurs in aggregates with cosalite, native bismuth and tetradymite group minerals. An important feature of lillianite from the sulphotelluride association is exsolution lamellae, visible as darker and lighter phases observed with BSE imaging (Fig. 3E). Cosalite was found in this study in association with Bi-sulphotellurides and other Bi-sulphosalts. It occurs as intergrowths with galena (Fig. 3C,E,F), or the Sb-rich lillianites and the kobellite homologues series (Fig. 3G,H). Jamesonite occurs as needles or larger irregular aggregates replacing other minerals, like galena or izoklakeite-giesenite and cosalite (Fig. 3H).

Sulphotelluride association

Four different chemical compositions of sulphotellurides were identified; primarily joséite-A (ideally Bi_4TeS_2), joséite-B (ideally Bi_4Te_2S), and two phases (of composition close to $(Bi,Pb)_2(TeS)_2$ and $(Bi,Pb)_{2.5}Te_{1.5}S_{1.5}$) that could not be unambiguously assigned to any known minerals, and are described below as phase A, and phase B. Chemical compositions from representative EPMA analyses are presented in Tables 1 and 2. The range of chemical compositions of the phases recognized are plotted in Figure 4. The EPMA data do not fall exactly on theoretical end-member values, and are rather dispersed on the plot.

The joséite-A EPMA data plot on a line, starting with an ideal stoichiometric joséite-A chemical composition and continuing in the direction of increased S, Pb, and Bi contents (Fig. 4). The Pb content in phases assigned to the joséite-A group are from 2.69 to 9.52 wt. %, Bi varies from 75.93 to 79.31 wt. %, Te from 7.63 to 11.83 wt. % and S from 6.39 to 7.32 wt. % (Table 1). The Ag content is up to 0.05 wt. %, Se up to 0.15 wt. % and Sb up to 0.34 wt. %.

Joséite-B has a similar trend to joséite-A through increased S, Pb, and Bi contents, towards the ideal Bi_3TeS composition. The Pb content in phases assigned to the joséite-B group are up to 2.58 wt. %, Bi varies from 68.12 to 79.35 wt. %, Te from 14.92 to 24.18 wt. % and S from 2.81 to 3.94 wt. %. The Ag content is up to 0.05 wt. %, of Se up to 0.20 wt. % and Sb up to 0.68 wt. %. Phase A has a chemical composition between telluronevskite and ingodite (Fig. 4). Its general structural formula is $(Bi,Pb)_2(TeS)_2$. The (Bi+Pb) to (S+Te+Se) ratio is 1:1. The scatter plot with data for Phase A and Phase B falls away from aleksite sub-group line as was proposed by Cook et al. (2007b) on their figure 6 therein so we are not considering our phases as aleksite sub-group minerals.

Compositions assigned to phase A have 5.50–20.37 wt. % Pb, 51.71–74.55 wt. % Bi, 16.65–22.82 wt. % Te, and 5.32–9.95 wt. % S (Table 2). Phase A contains up to 0.16 wt. % of Ag.

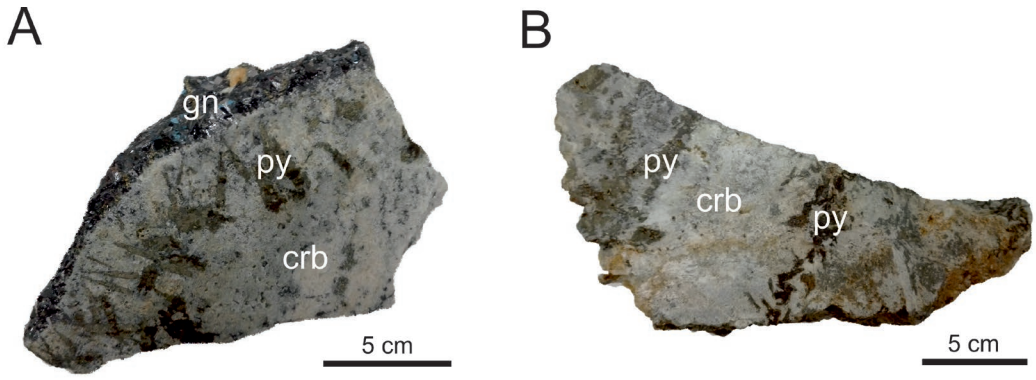

Fig. 2. Host rock samples for bismuth-telluride association occurring between elongated pyrite (py) crystals in the carbonate matrix (crb). **A** — Sample from orebody No. 140 overgrown by coarse-grained galena (gn); **B** — Sample from orebody No. 141.

Fig. 3. BSE images of the sulphotelluride Bi–Sb–Pb–Te–S association. **A** — Cosalite (cos) aggregate with telluride minerals (white inclusions). **B** — Detail of image A. Telluride inclusions composed of phases A and B. **C** — Aggregate of cosalite (cos) replacing galena (gn) with tetradymite minerals: ikunolite (ikn), joséite-B (josB) and native bismuth (Bi). **D** — Detail of image C. Joséite-A (josA) intergrown with joséite-B (josB) and native bismuth (Bi). **E** — Lillianite exsolutions. White needles with high Ag content, and darker needles with low Ag content. Gn – galena, cos – cosalite, ikn – ikunolite, josB – joséite-B. **F** — Cosalite (cos) and native bismuth (Bi) replacing galena (gn). josA – joséite-A, ikn – ikunolite, L – lillianite. **G** — Aggregate composed of kobellite-tintinaite (kob), izoklakeite-giessenite (izo), cosalite (cos), and galena (gn). **H** — jamesonite (jm) replacing cosalite (cos) and izoklakeite-giessenite (izo). Kob – kobellite-tintinaite.

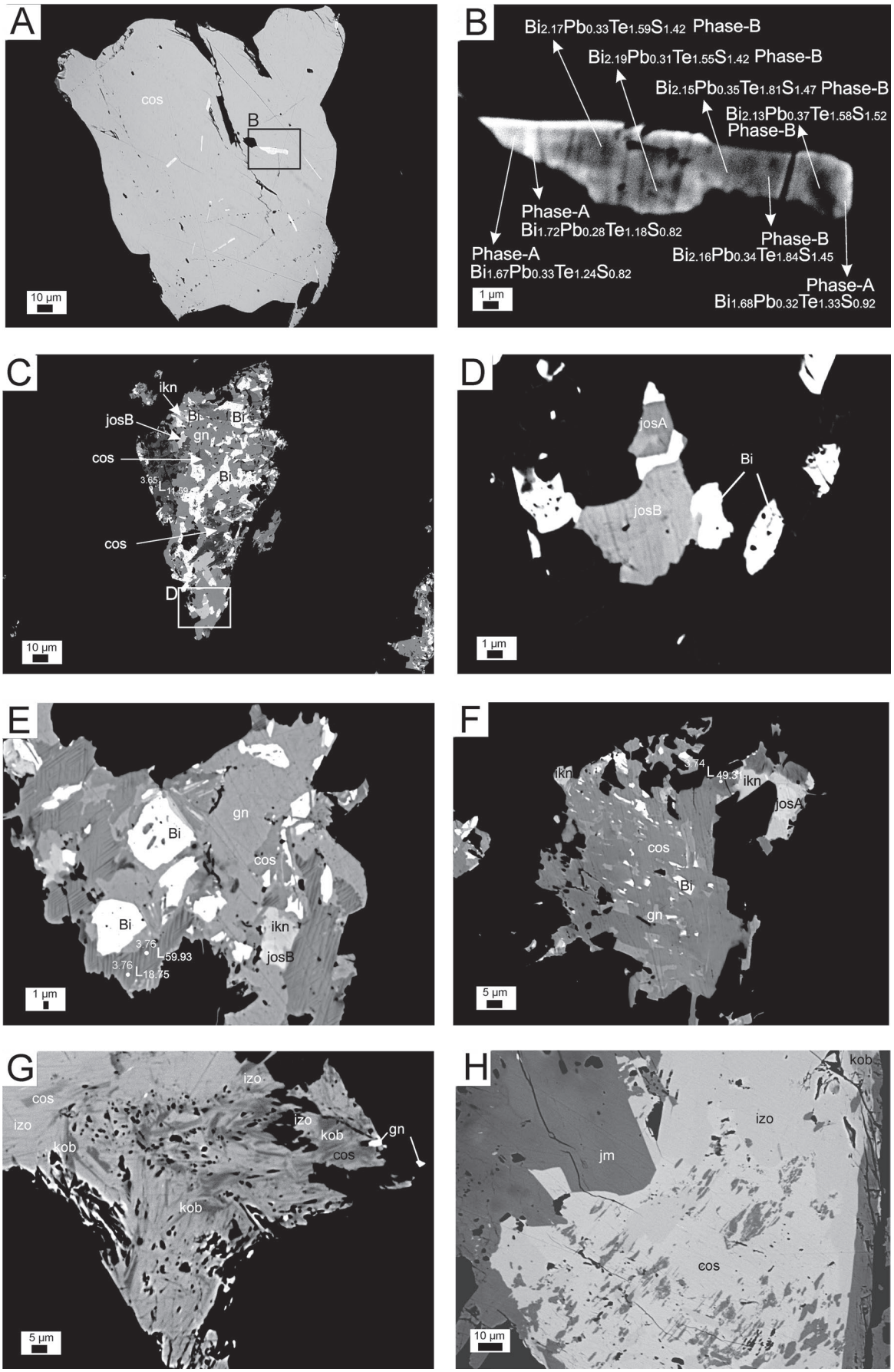
A
cos
B
10 µm
B
Bi2.17Pb0.33Te1.59S1.42 Phase-B
Bi2.19Pb0.31Te1.55S1.42 Phase-B
Bi2.15Pb0.35Te1.81S1.47 Phase-B
Bi2.13Pb0.37Te1.58S1.52 Phase-B
Phase-A Bi1.72Pb0.28Te1.18S0.82
Phase-A Bi1.67Pb0.33Te1.24S0.82
Phase-B Bi2.16Pb0.34Te1.84S1.45
Phase-A Bi1.68Pb0.32Te1.33S0.92
1 µm
C
ikn
josB
Bi
Bi
gn
cos
Bi
3.65
L 11.59
cos
D
10 µm
D
josA
Bi
josB
1 µm
E
gn
Bi
cos
Bi
ikn
3.75
L 59.93
josB
3.76
L 18.75
1 µm
F
ikn
3.74
L 49.31
ikn
josA
cos
Bi
gn
5 µm
G
izo
cos
izo
izo
kob
gn
kob
cos
kob
5 µm
H
kob
izo
jm
cos
10 µm

Phase B has a chemical composition close to $(Bi,Pb)_{2.5}Te_{1.5}S_{1.5}$. The (Bi+Pb) to (S+Te+Se) ratio is 2.5:3, and this telluride has the highest Te content, that is in the range between 25.87 and 29.33 wt. % (Table 2). Lead varies between 8.80–10.19 wt. %, Bi between 55.95 and 61.44 wt. %, and S between 5.85 and 6.28 wt. %.

Ikunolite

Ikunolite (ideally $Bi_4(S,Se)_3$) is a tetradymite-group mineral previously described in Stan Terg in association with other Bi-minerals and joséite-A (Kołodziejczyk et al. 2015). Previous analyses indicated a good correlation between Pb and Bi in ikunolite, babkinite and the intermediate phases, suggesting a possible ikunolite-babkinite solid solution, with very limited Se for S substitution (Kołodziejczyk et al. 2015). Ikunolite-babkinite solid solutions revealed up to 0.25 wt. % Te and up to 0.3 wt. % Ag (Kołodziejczyk et al. 2015).

Ikunolite within the sulphotelluride association (this study), occurs mostly as intergrowths with the above described sulphotellurides and with lillianite, cosalite, native bismuth, and galena. Representative EPMA analyses of ikunolite are presented in Table 1. Its Pb content varies between 0.99 and 23.40 wt. %, and there is a positive correlation trend towards the babkinite composition, however only up to 0.9 apfu of Pb. The ikunolite contains Ag up to 0.13 wt. %, Sb up to 0.11 wt. %, and up to 1.22 wt. % Te. Selenium up to 0.15 wt. % was detected in some analyses. Ikunolite has a composition similar to ikunolite from the skarn-hosted and skarn-free mineral association (e.g. Kołodziejczyk et al. 2015), with Pb concentrations up to 23 wt. % (for intermediate ikunolite-babkinite phases).

Cosalite

Cosalite was previously described from Stan Terg by Terzić et al. (1974, 1975), with a single EPMA analysis indicating chemical composition close to ideal, with 0.27 apfu of Sb, and up to 0.01 apfu of Ag.

Representative EPMA analyses of cosalite, together with analyses for coexisting galena, are presented in the Table 3. Cosalite has up to 0.72 apfu of Cu+Ag (1.50 wt. %), and up to 3.94 apfu of Sb (13.57 wt. %), thus resulting in a shift of chemical composition of the Stan Terg cosalite towards increased Sb content (Fig. 5). Binary plots with compositional data for Stan Terg cosalite for Cu+Ag, and Pb, Bi, Bi+Sb are presented in Figure 6. There is a good correlation between Sb and Bi over a wide range of Sb/(Sb+Bi) ratios (Fig. 6D).

Table 1: Representative EPMA analyses and atomic proportions for tetradymite group minerals from the sulphotelluride association: ikunolite (1–4), joséite-A (5–6), joséite-B (7–11) in the Stan Terg deposit.

	1	2	3	4	5	6	7	8	9	10	11
Pb	0.77	1.08	4.28	10.22	7.34	3.79	0.61	1.55	0.19	0.71	0.29
Fe	0.32	<MDL	0.05	0.04	0.17	0.02	0.07	0.12	0.03	0.47	0.03
Cu	0.03	<MDL	<MDL	<MDL	<MDL	<MDL	<MDL	<MDL	0.03	0.01	<MDL
Ag	0.04	0.13	0.08	0.01	<MDL	0.02	0.01	<MDL	0.03	<MDL	0.05
Sb	0.03	<MDL	0.04	0.09	0.22	0.25	0.37	0.36	0.46	0.42	0.46
Bi	89.37	89.54	86.42	79.8	78.21	79.49	75.93	75.89	76.87	76.21	76.78
Te	0.83	1.16	0.16	0.74	7.76	10.47	21.87	20.69	21.12	21.12	21.32
Se	0.11	0.10	0.04	<MDL	<MDL	0.07	<MDL	<MDL	0.09	<MDL	0.01
S	10.04	10.21	10.19	10.34	6.91	6.74	2.89	3.07	3.04	3.03	3.03
TOTAL	101.54	102.22	101.26	101.24	100.61	100.85	101.75	101.68	101.86	101.97	101.97
	Chemical formula based on sum of 7 atoms										
Pb	0.03	0.05	0.19	0.45	0.36	0.18	0.03	0.08	0.01	0.04	0.02
Fe	0.05	–	0.01	0.01	0.03	0.00	0.01	0.02	0.01	0.09	0.01
Cu	0.00	–	–	–	–	–	–	–	0.00	0.00	–
Ag	0.00	0.01	0.01	0.00	–	0.00	0.00	–	0.00	–	0.01
Sb	0.00	–	0.00	0.01	0.02	0.02	0.03	0.03	0.04	0.04	0.04
Bi	3.94	3.93	3.83	3.51	3.79	3.83	4.02	4.01	4.05	3.99	4.05
Te	0.06	0.08	0.01	0.05	0.62	0.83	1.90	1.79	1.82	1.81	1.84
Se	0.01	0.01	0.00	–	–	0.01	–	–	0.01	–	0.00
S	2.89	2.92	2.94	2.97	2.19	2.12	1.00	1.06	1.05	1.03	1.04

Notes: <MDL = below the minimum detection limit

Table 2: EPMA analyses of phase A (1–4) and phase B (5–8) from the sulphotelluride association in the Stan Terg deposit.

	1	2	3	4	5	6	7	8
Pb	10.31	12.01	10.41	17.11	9.02	8.80	8.32	8.80
Fe	0.02	0.06	0.04	0.36	0.02	0.02	0.02	0.12
Cu	<MDL	0.01	0.01	<MDL	<MDL	0.01	<MDL	0.01
Ag	0.01	0.05	0.02	0.09	0.04	<MDL	0.01	<MDL
Sb	0.14	0.20	0.20	0.40	0.23	0.21	0.19	0.23
Bi	69.27	62.34	63.91	56.41	55.95	59.32	59.54	56.32
Te	13.88	18.60	18.67	17.86	28.75	26.48	25.68	29.33
Se	0.03	<MDL	0.09	0.04	<MDL	0.05	<MDL	0.11
S	6.73	7.06	6.73	8.11	5.86	5.96	5.93	5.79
TOTAL	100.18	100.33	100.08	100.38	99.87	100.85	99.69	100.71
	Chemical formula based on sum of 2 cations				Chemical formula based on sum of 2.5 cations			
Pb	0.26	0.33	0.28	0.47	0.35	0.33	0.31	0.34
Fe	0.00	0.01	0.00	0.04	0.00	0.00	0.00	0.00
Cu	–	0.00	0.00	–	–	0.00	–	0.00
Ag	0.00	0.01	0.01	0.00	0.00	–	0.00	–
Sb	0.01	0.01	0.01	0.02	0.02	0.01	0.01	0.02
Bi	1.74	1.67	1.72	1.53	2.15	2.17	2.19	2.16
Te	0.57	0.82	0.82	0.79	1.81	1.59	1.55	1.84
Se	0.00	–	0.01	0.00	–	0.01	–	0.01
S	1.10	1.24	1.18	1.44	1.47	1.42	1.42	1.45

Notes: <MDL = below the minimum detection limit

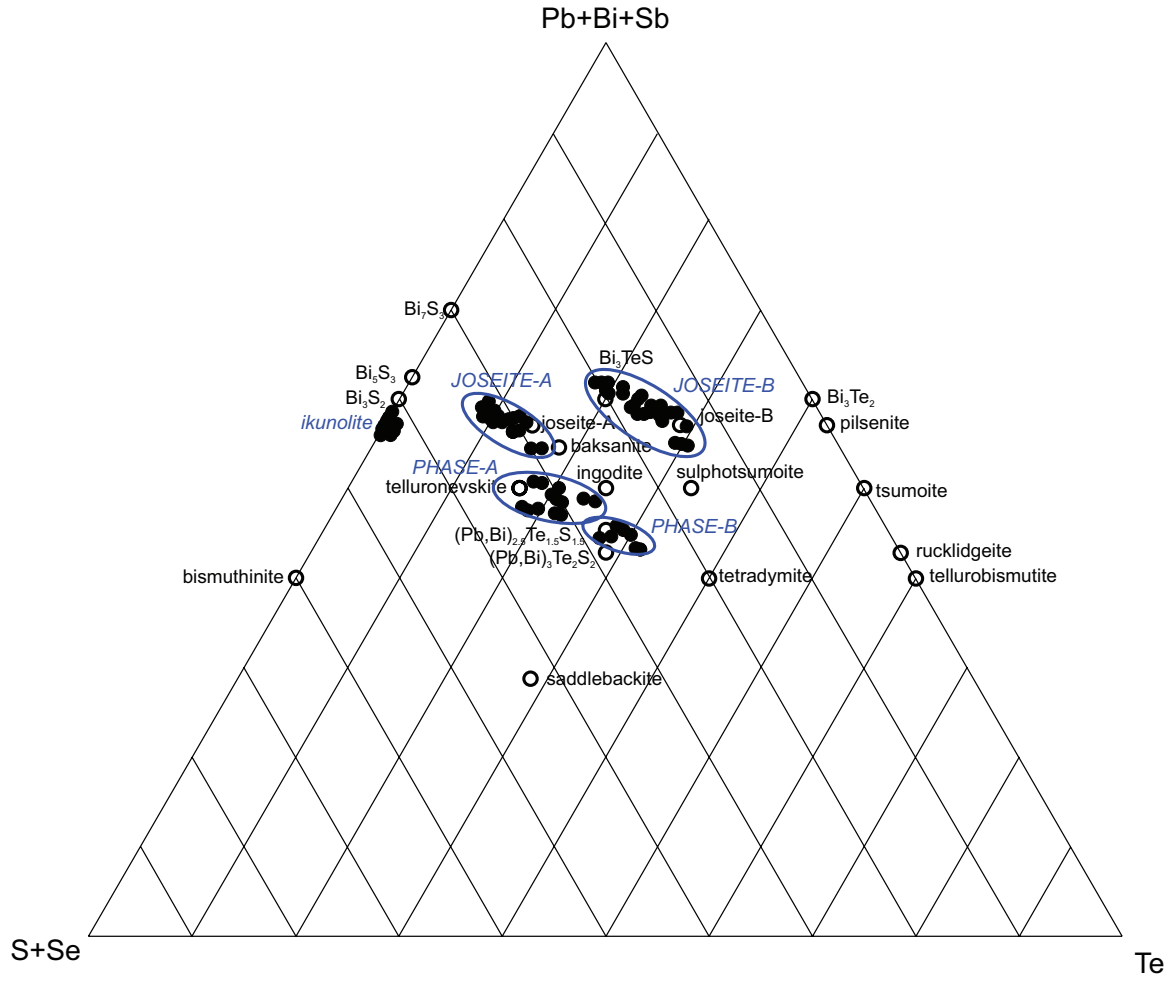

Fig. 4. Ternary plot Bi+Pb+Sb vs S+Se vs Te of Bi-sulphotelluride minerals from the Stan Terg mine. Open circles: minerals ideal end member chemical compositions; solid black symbols: chemical compositions of minerals from the Stan Terg deposit.

Sb-rich lillianite

Lillianite (N=4) and heyrovskite (N=7), two members of the lillianite homologous series, were recently reported at the Stan Terg deposit in association with other Bi-sulphosalts, galena and arsenopyrite (Kołodziejczyk et al. 2015). They contain up to 0.2 wt. % of Sb.

In contrast, lillianite accompanying the Bi-sulphotellurides has a different chemical composition with significantly higher Sb content (up to 11.50 wt. %), and also a higher Ag content (up to 5.10 wt. %). This Sb-rich lillianite has been found in the samples from the orebody 141, as aggregates intergrown with galena, native bismuth, cosalite, and tetradymite group minerals.

Table 3: Representative EPMA analyses and atomic proportions for cosalite (1–6) and coexisting galena (7–9) from Stan Terg.

	1	2	3	4	5	6	7	8	9
Pb	40.00	40.58	40.65	40.21	41.67	43.49	84.77	85.47	84.89
Fe	0.59	0.21	0.25	0.27	0.26	0.64	0.03	0.03	0.05
Cu	0.32	0.16	0.17	0.14	0.16	0.98	<MDL	<MDL	0.02
Ag	0.89	0.48	0.44	0.65	0.67	0.52	0.58	0.18	0.32
Sb	0.41	3.47	3.89	6.14	7.61	13.57	0.03	<MDL	<MDL
Bi	41.42	37.47	37.21	34.40	31.79	22.34	2.52	1.31	1.51
Mn	<MDL	0.14	0.06	0.16	0.21	0.00	0.01	<MDL	0.01
Te	0.04	0.07	0.03	<MDL	0.13	0.04	0.03	0.14	<MDL
S	16.03	16.70	16.65	16.99	17.21	18.13	13.50	13.05	13.42
TOTAL	99.70	99.28	99.35	98.96	99.71	99.71	101.47	100.18	100.22
	Chemical formula based on anions = 20						Chemical formula based on 2 atoms		
Pb	7.52	7.51	7.55	7.33	7.48	7.42	0.96	0.98	0.97
Fe	0.42	0.15	0.17	0.19	0.18	0.40	0.00	0.00	0.00
Cu	0.21	0.10	0.11	0.09	0.10	0.55	–	–	0.00
Ag	0.33	0.17	0.16	0.23	0.23	0.17	0.01	0.00	0.01
Sb	0.13	1.09	1.07	1.90	2.32	3.94	0.00	–	–
Bi	7.92	6.88	6.85	6.21	5.66	3.78	0.03	0.01	0.02
Mn	–	0.01	0.04	0.11	0.14	0.00	0.12	–	0.00
Te	0.01	0.02	0.01	–	0.04	0.01	0.00	0.00	–
S	19.99	19.98	19.99	20.00	19.96	19.99	0.98	0.97	0.99

Notes: <MDL = below the minimum detection limit, Se was below the minimum detection limit in all analyses

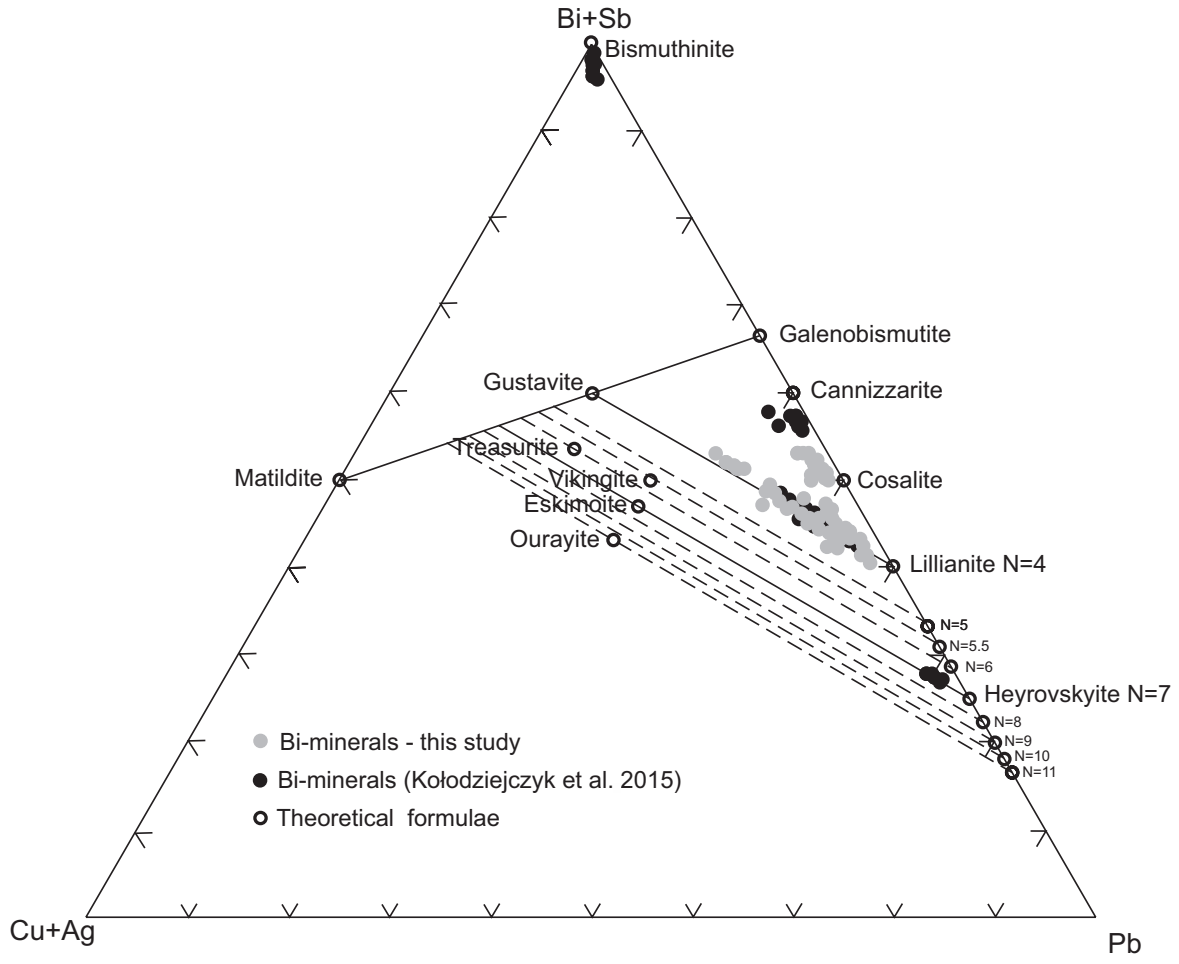

Fig. 5. Ternary plot Cu+Ag vs Bi+Sb vs Pb of bismuth sulphosalts — new data and previously described phases in the Stan Terg mine.

Representative EPMA data are presented in Table 4. For all analysed grains the N number was calculated with values around 4 (e.g., 3.70–4.14), which means the only member of the lillianite homologous series present in the association is lillianite, 4L. The molar percentage of the gustavite member ranges between 8.08 and 55.60 mol. %, whereas the silver content in apfu (x) ranges between 0.08 and 0.51 (Fig. 5).

By comparing the chemical composition of exsolution lamellae in lillianite we conclude that the lighter phases are described as $^{3.76}L_{18.75}$, with x value=0.17, whereas the darker zones are enriched in Ag, and their composition is around $^{3.76}L_{59.93}$, with x=0.47 (both measured with an electron beam diameter below 1 μm). One analysis with a 4 μm electron beam, could be assigned to an unexsolved phase that was around $^{3.83}L_{26.28}$, with x=0.24.

X-ray maps (Fig. 7) show a lillianite aggregate from the sulphotelluride association, partly replaced by galena, ikunolite, native bismuth, and Bi-sulphotellurides (joséite-A, joséite-B). Copper and Pb distribution are uniform throughout the lillianite aggregates, whereas Ag and Sb are slightly increased at the edges. Sulphotellurides are intergrown with ikunolite, or occur as inclusions in galena or lillianite.

Kobellite homologous series

Recently, the presence of izoklakeite-giessenite members of the kobellite homologous series in the Stan Terg deposit was reported by Kolodziejczyk et al. (2015). In the sulphotelluride association (samples from 140 and 141 orebodies), phases that represent both members, for example, izoklakeite-giessenite (N=4), as well as kobellite-tintinaite series (N=2) were identified. However, in this association izoklakeite-giessenite phases are dominant.

Kobellite homologous series phases occur in the sulphotelluride association together with Bi-rich jamesonite, Sb-cosalite (up to Sb 3.94 apfu), and minor galena (Fig. 3G,H). The chemical composition of these minerals is presented in Table 5 and in Figure 8.

An almost ideal Bi↔Sb substitution trend is visible in both series (Fig. 8A). The Sb/(Sb+Bi) ratio is 0.47–0.51 in the kobellite-tintinaite series and 0.31–0.51 in the izoklakeite-giessenite series. The Ag content is insignificant, and

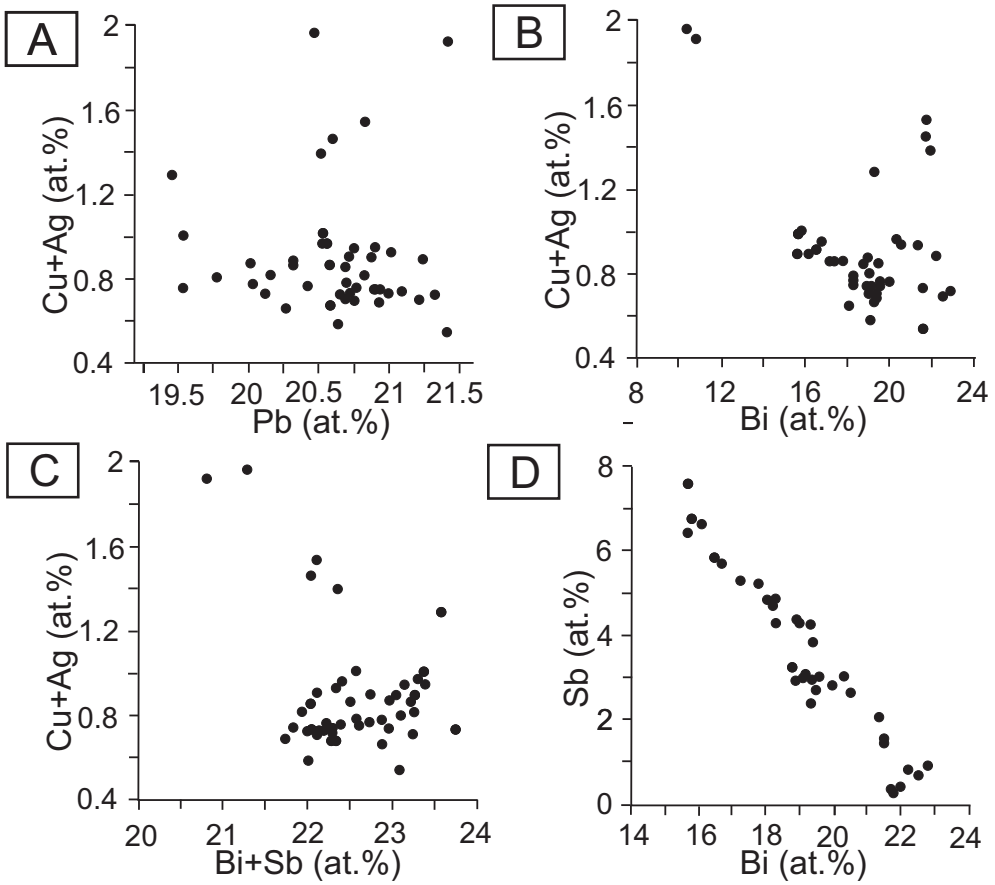

Fig. 6. Binary plots showing chemical composition of cosalite from the Stan Terg deposit. **A** — Cu vs Ag at. %; **B** — Cu+Ag vs Pb at %; **C** — Cu+Ag vs Bi at. %; **D** — Cu+Ag vs Bi+Pb at. %.

corresponds to 0.1 apfu and 0.5 apfu on average in both series, respectively.

Bi-rich jamesonite

Jamesonite from the Stan Terg deposit was found in samples from the 140 orebody. Representative EPMA data are presented in Table 6. Chemical composition data indicates that the Bi content in all phases measured reaches up to 21 wt. %, which corresponds to 0.85 to 2.30 apfu in the chemical formula.

Table 4: Representative EPMA analyses and atomic proportions for Sb-rich lillianite from sulphotelluride association in the Stan Terg deposit.

	1	2	3	4	5	6	7	8	9	10
Pb	37.86	34.66	40.52	38.75	40.53	48.67	46.04	48.48	41.35	35.02
Fe	<MDL	0.05	0.09	0.04	0.90	0.06	0.16	1.32	0.16	0.49
Cu	0.01	<MDL	<MDL	<MDL	0.01	<MDL	<MDL	<MDL	0.02	0.08
Ag	3.87	4.60	3.24	3.48	3.05	1.00	1.26	1.26	3.60	5.10
Sb	0.34	0.36	0.50	0.62	0.68	1.21	1.24	1.89	4.99	11.50
Bi	43.14	45.19	40.15	42.76	40.52	33.99	34.50	33.24	35.39	29.22
Te	<MDL	<MDL	<MDL	0.01	<MDL	0.08	0.04	<MDL	<MDL	<MDL
Se	<MDL	<MDL	<MDL	<MDL	<MDL	<MDL	<MDL	<MDL	0.07	<MDL
S	16.29	16.20	16.11	16.09	15.97	15.47	15.80	15.60	16.16	17.88
TOTAL	101.51	101.06	100.61	101.75	101.66	100.48	99.04	101.79	101.74	99.29
	Chemical formula based on (Pb+Bi+Ag) = 5									
Pb	2.15	1.96	2.34	2.21	2.34	2.89	2.78	2.89	2.48	2.37
Bi	2.43	2.54	2.30	2.41	2.32	2.00	2.07	1.97	2.11	1.96
Ag	0.42	0.50	0.36	0.38	0.34	0.11	0.15	0.14	0.41	0.66
S	5.98	5.93	6.01	5.92	5.96	5.93	6.18	6.01	6.26	7.82
N	3.93	3.86	4.08	3.83	3.94	4.11	4,00	4.16	4.01	3.82
mol%	42.75	51.90	34.83	39.62	33.92	10.83	14.26	13.24	37.52	55.60
x	0.41	0.48	0.36	0.36	0.33	0.11	0.14	0.14	0.38	0.51

Notes: <MDL = below the minimum detection limit

Discussion

The Bi–Pb–Sb–S–Te association discussed in the present study differs from that described previously by Kołodziejczyk et al. (2015) (e.g., skarn-, and skarn-free breccias filling types), in that it is enriched in tellurides. This association was found in the external parts of the skarn orebodies as aggregates between dispersed pyrite crystals in the gangue carbonate host rock. The source of the Bi–Pb–Sb–S–Te mineralization is likely to be the same as for the two types described above, and the Bi-sulphotelluride

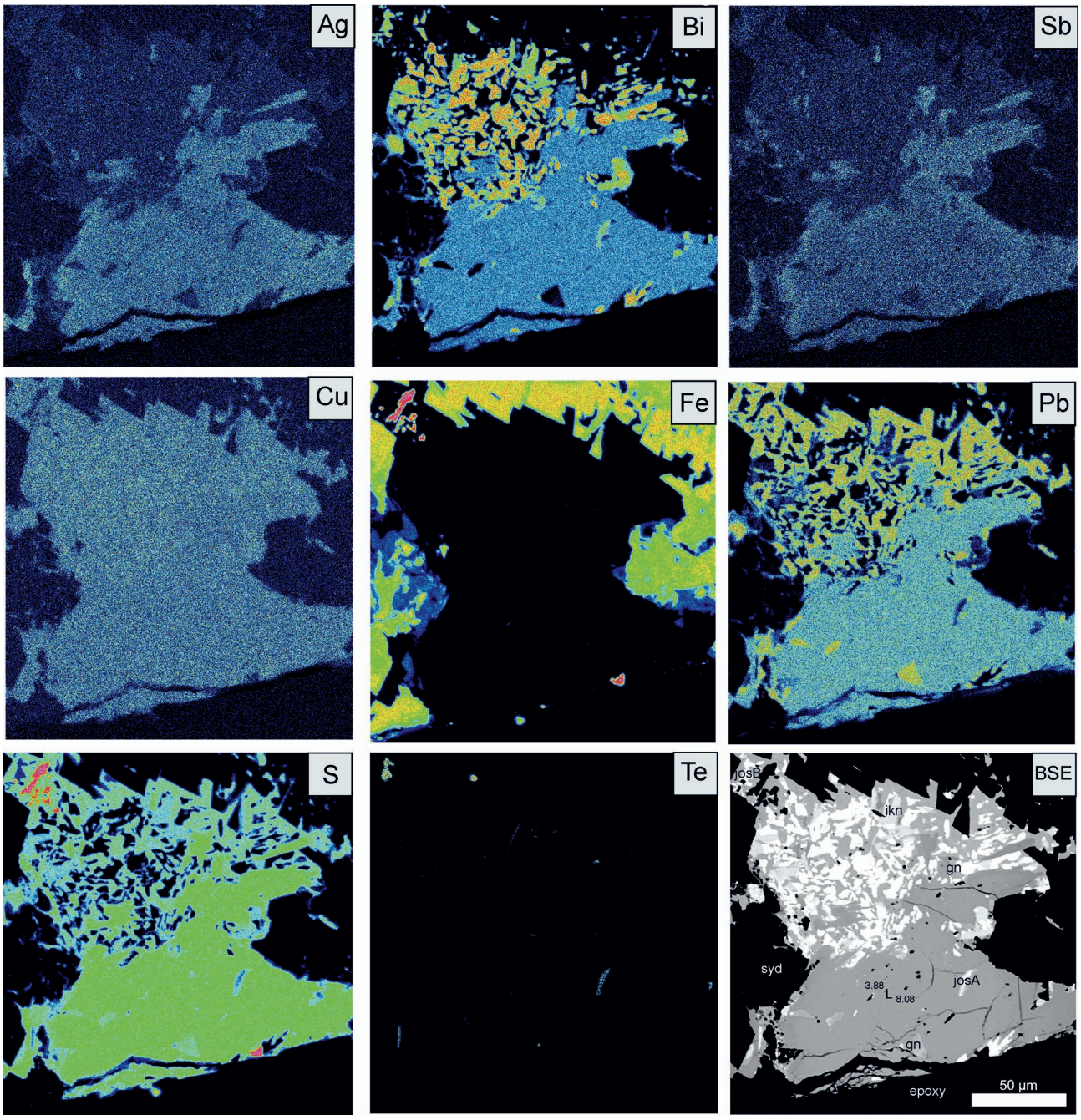

Fig. 7. EPMA X-Ray maps (AgLα, BiMα, SbLα, CuKα, FeKα, PbMα, SKα, TeLα) of lillianite intergrowth (L) with galena (gn), native bismuth (Bi), ikunolite (ikn) and Bi-tellurides: joséite A (josA), and joséite B (josB).

association was probably the result of precipitation from fluids that derived from the main skarn orebody and then migrated into the host rocks around the skarn mineralization, resulting in skarn-free local enrichment in tellurides.

Identification of tetradymite group species

In the absence of structural data that were beyond the scope of this study (e.g., X-ray diffraction, Raman spectroscopy, nanoscale electron diffraction on a TEM platform), for the identification of telluride phases present we propose the following approaches: 1) substitution; 2) the presence of submicroscopic PbS layers; 3) incorporation of Bi–(Pb) modules.

The "substitution" approach may be considered valid because of the absence of Pb in natural, ideal chemical compositions of joséite-B (Bi_4TeS_2), and protojoseite (Bi_3TeS). Similar to the discussion by Cook et al (2007a), this trend suggests Bi↔Te substitution (or "disorder"?) and described by those authors as compounds close to Bi_3TeS composition

could be disordered members of the tsumoite–ingodite–nevskite series. They do not rule out, however, the possibility of stable minerals with this stoichiometry.

Our compositional data for joséite-A and joséite-B, trend in the direction of the "protojoseite line", marked according to its stoichiometric formula of $Bi_3(Te,S)_2$, indicating a wide compositional range of Te and S in this phase (Fig. 9A). Some of the data plot directly on this line. Protojoseite remains a questionable mineral species (e.g., Jambor 1984) and its stoichiometry was reported as 3:2 and 4:3, or the phase was suggested to be a non-stoichiometric joséite-B or joséite-A (Cook et al. 2007a). Zav'yalov & Begizov (1983) suggested a narrow compositional field for protojoseite with the general formula $Bi_{3+x}Te_{1-x-y}S_{1+y}$, where $-0.02<x<0.14$ and $-0.05<y<0.17$, which may explain the Bi:(Te+S) variations that were observed.

Table 5: Representative EPMA analyses and atomic proportions for kobellite homologous series minerals from sulphotelluride association: kobellite-tintinaite (1–5), izoklakeite-giessenite (6–10) in the Stan Terg deposit.

	1	2	3	4	5	6	7	8	9	10
Pb	38.04	37.54	37.7	39.29	38.72	48.01	48.13	49.18	49.23	50.06
Fe	0.97	0.98	0.94	0.89	0.94	0.46	0.38	0.34	0.28	0.47
Cu	0.97	0.97	0.98	1.01	1.01	0.72	0.73	0.82	0.93	0.92
Ag	0.18	0.17	0.12	0.19	0.16	0.36	0.41	0.56	0.62	0.61
Sb	13.68	14.35	14.69	14.93	15.11	4.75	4.78	8.38	10.89	13.36
Bi	26.55	26.06	25.53	24.35	25.05	28.37	28.97	23.41	20.55	16.3
Mn	0.02	0.01	<MDL	<MDL	<MDL	0.02	<MDL	0.02	0.01	0.17
Te	<MDL	<MDL	<MDL	0.01	<MDL	<MDL	0.18	<MDL	0.05	<MDL
S	18.59	18.79	18.79	18.82	18.79	16.46	16.47	16.99	17.2	17.45
TOTAL	98.99	98.86	98.75	99.48	99.77	99.15	100.05	99.71	99.74	99.32
	Chemical formula based on (Pb+Bi+Ag+Sb) = 26					Chemical formula based on (Pb+Bi+Ag+Sb) = 46				
Pb	11.24	11.08	11.11	11.45	11.24	26.01	25.81	25.79	25.35	25.55
Fe	1.06	1.07	1.03	0.96	1.01	0.93	0.75	0.66	0.53	0.89
Cu	0.94	0.95	0.96	0.98	0.97	1.30	1.30	1.43	1.58	1.56
Ag	0.10	0.10	0.07	0.11	0.09	0.37	0.42	0.56	0.61	0.60
Sb	6.88	7.20	7.37	7.41	7.46	4.38	4.36	7.48	9.54	11.6
Bi	7.78	7.63	7.46	7.04	7.21	15.24	15.40	12.17	10.49	8.25
Mn	0.02	0.01	–	–	–	0.04	–	0.05	0.01	0.32
Te	–	–	–	0.00	–	–	0.16	–	0.05	–
S	35.49	35.84	35.79	35.44	35.25	57.64	57.07	57.55	57.23	57.56
N	2.11	2.06	2.05	2.19	2.11	3.97	3.97	4.14	4.04	4.07
x	0.47	0.47	0.48	0.50	0.49	0.58	0.63	0.68	0.75	0.63

Notes: <MDL = below the minimum detection limit, Se was below the minimum detection limit in all analyses

Results similar to those obtained in the present study, for coexisting joséite-B and "protojoseite", were reported by Zav'yalov & Begizov (1983), and later by Cook et al. (2007a). However, in these studies, the compositional data differ noticeably for both species, and the results do not overlap with fields for ideal stoichiometric joséite-A and joséite-B.

Compositions which are apparently non-stoichiometric can be readily interpreted in terms of (disordered or ordered) finest-scale intergrowths, as described by Cook et al. (2007a,b): The "PbS sublayers" approach is supported by the three visible trends on the Pb+Bi+Sb vs S+Se vs Te diagram (Fig. 9B): 1st from Bi_7S_3–to joséite-B; 2nd from Bi_5S_3–joséite-A–sulphotsumoite–to tellurobismutite; and 3rd from ikunolite–phase A with formula $(Bi,Pb)_2(TeS)_2$ – phase B with formula $(Bi,Pb)_{2.5}Te_{1.5}S_{1.5}$ – to tetradymite. Those lines can support the admixture of tellurides with submicroscopic intergrown layers of PbS, so the analyses fall between the phases mentioned above on that diagram.

Although unnamed Phases A and B plot away from the aleksite sub-group line (e.g. Cook et al. 2007a) and thus cannot be explained in terms of aleksite sub-group phases, the observed compositions could be alternatively, attributed to submicroscopic intergrowths of tetradymite units with Pb–Bi sulphotellurides.

Finally, lattice-scale intergrowths between members of the tetradymite group (e.g. consideration of Bi–Pb modules approach), similar to those described by Ciobanu et al. (2009b) could also explain the composition of unnamed phases A and B.

Sb-rich cosalite

Cosalite is a common Bi-sulphosalt, ideally $Pb_2Bi_2S_6$, with several possible substitutions, including Ag, Cu, or Sb. Recently Topa & Makovicky (2010) proposed the following substitution mechanisms in cosalite: 1) Ag+Bi↔2Pb at the Me1 *site;* and 2) 2(Cu+Ag)↔Pb. They proposed these as a result of the creation of vacancies in the Bi-containing octahedral Me2 *site* accompanied by a progressive occupancy of two triangular faces of this octahedron by Cu+Ag [i.e., Bi↔2(Cu + Ag)]. This in turn is combined with the replacement of Pb in the adjacent Me1 octahedron by Bi. Their two substitution mechanism combinations explain the closely followed chemical relationship above.

Antimony for Bi substitution in cosalite is easier to explain. Antimonian cosalite (up to Sb = 6.89 wt. %) was first described by Lee at al. (1993) from the Dunjeon Au mine (Japan). Cosalite with high Sb contents was also reported from Bacúch (Pršek & Chovan 2001; Pršek 2008) and from Brezno-Hviezda (Pršek et al. 2008) in the Low Tatras, Slovakia, with Sb contents reaching values of up to 0.72 and 3.33 wt. %, respectively. Sb-bearing cosalite with up to 4.33 wt. % of Sb was also described by Cook (1997) from the Bi sulphosalt-bearing, hydrothermal Pb–Zn mineralization at Baia Borşa, Romania.

The cosalite from Stan Terg was previously described by Terzić et al. (1974, 1975). He indicated, based on XRD and EPMA results, that cosalite has up to 0.27 apfu Sb and up to 0.01 apfu Ag. The composition of cosalite measured by Terzić falls between the results of the present study (Fig. 7). We

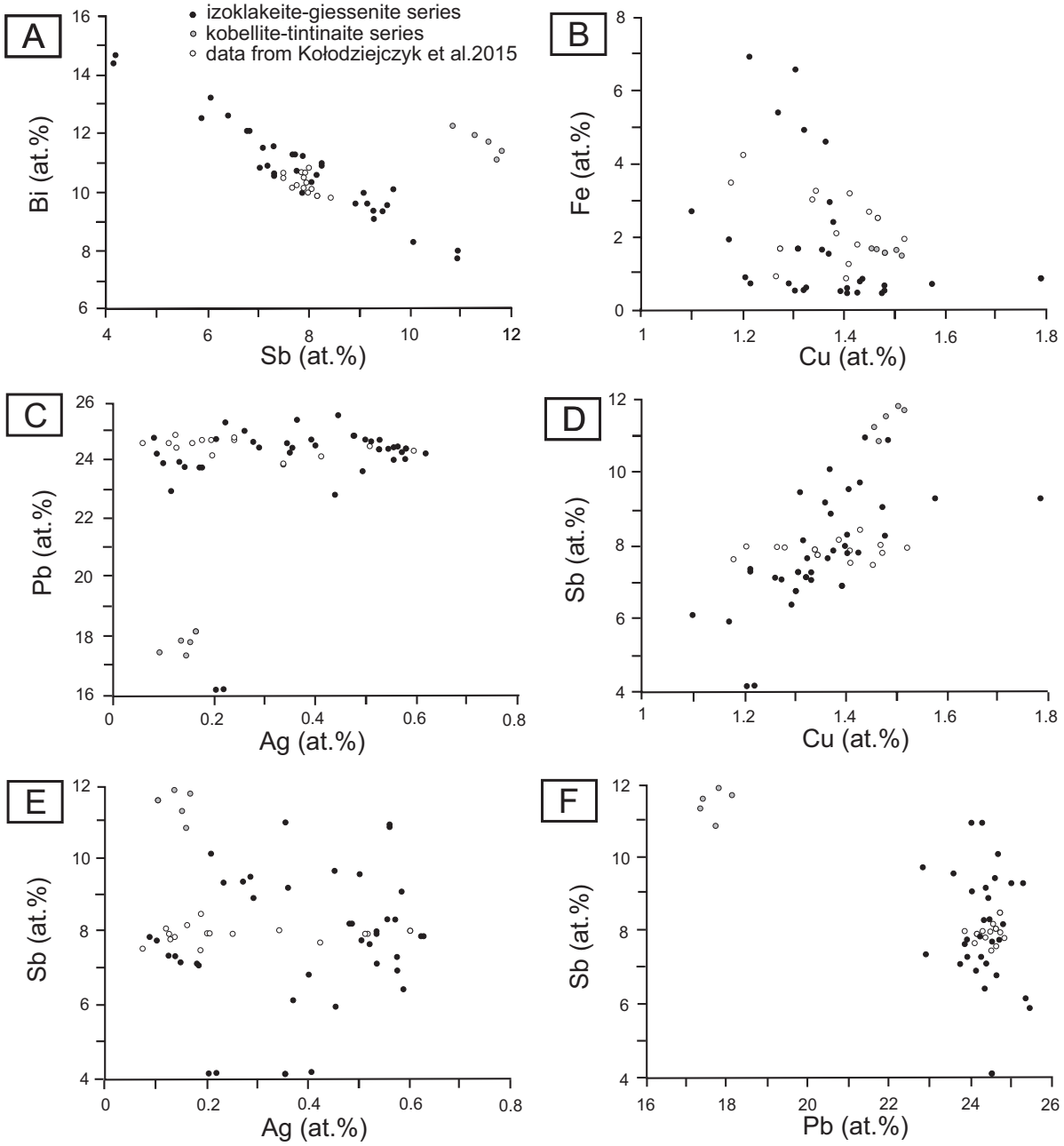

Fig. 8. Binary plots showing chemical composition of kobellite homologous series from the sulphotelluride association at the Stan Terg deposit. **A** — Bi vs Sb at. %, **B** — Fe vs Cu at. %, **C** — Pb vs Ag at. %, **D** — Sb vs Cu at. %, **E** — Sb vs Ag at. %, **F** — Sb vs Pb at. %.

suggest that the chemical composition of Stan Terg cosalite is more complex than previously thought and depends on the Ag+Cu and Bi+Sb contents. The cosalite composition from Stan Terg is compared in Figure 10 to other Sb-rich cosalites from different localities. The antimony content in the Stan Terg cosalites is relatively high, but Cu+Ag substitution is relatively limited.

Bi-rich jamesonite

Bi-rich jamesonite with significant high Bi content was described from several hydrothermal vein occurrences in Eastern Europe: Pršek et al. (2008) described jamesonite with up to 2.41 apfu Bi, occurring with kobellite, eclarite and sulphosalts of the bismuthinite-aikinite group, from Brezno-Hviezda, Slovakia. In the Úhorná locality (Slovakia) the Bi content in jamesonite reaches 1.25 apfu, and this mineral was found in association with tetradymite group minerals, tintinaite, and bournonite (Pršek & Peterec 2008). Pršek (2004) reported from the Slovak Ore Mountains up to 1.20 apfu Bi in jamesonite, hosted in siderite veinlets and associated with kobellite homologues, jaskólskite, and Bi-bournonite. Substitution of Bi for Sb is common in jamesonite from all the above localities, which could suggest possible solid solution

with sakharovaite. Sakharovaite (ideally $FePb_4(Sb,Bi)_6S_{14}$) is considered to be either a Bi-rich variety of jamesonite, or a separate species, with Bi↔Sb substitution close to 50 at. % limit (Moëlo et al. 2008).

Table 6: Representative EPMA analyses and atomic proportions for representative Bi-rich jamesonite from the Stan Terg deposit (wt. %).

	1	2	3	4	5	6	7	8
Pb	38.71	38.81	38.58	38.33	37.58	37.81	36.91	37.07
Fe	2.51	2.66	2.79	2.94	2.39	2.36	2.48	2.22
Cu	0.01	<MDL	<MDL	<MDL	0.05	0.03	0.02	0.04
Ag	<MDL	<MDL	<MDL	<MDL	<MDL	<MDL	<MDL	0.01
Sb	28.75	26.77	26.06	25.39	22.24	21.78	20.41	19.57
Bi	8.15	10.94	11.11	13.16	16.21	17.66	20.24	21.05
Mn	<MDL	0.24	0.41	0.22	0.05	0.13	0.11	0.07
S	20.28	20.25	19.98	20.48	20.45	19.72	19.97	19.41
TOTAL	98.41	99.67	98.93	100.52	98.97	99.49	100.14	99.44
	Chemical formula based on heavy metals = 11							
Pb	4.05	4.03	4.01	3.97	4.11	4.09	4.01	4.09
Fe	0.98	1.02	1.08	1.13	0.97	0.95	1.00	0.91
Cu	0.00	–	–	–	0.02	0.01	0.01	0.02
Ag	–	–	–	–	–	–	–	0.00
Sb	5.12	4.73	4.61	4.47	4.14	4.01	3.77	3.67
Bi	0.85	1.13	1.15	1.35	1.76	1.90	2.18	2.30
Mn	0.00	0.09	0.16	0.08	0.02	0.05	0.04	0.03
S	13.73	13.58	13.42	13.69	14.45	13.79	14.01	13.83

Notes: <MDL = below the minimum detection limit, Se and Te were below the minimum detection limit in all analyses

Similar sulphotellurides in hydrothermal systems elsewhere

The sulphotelluride assemblages described from the Stan Terg deposit comprise various phases accompanying Bi-sulphosalts with low Ag contents. In addition, neither native gold nor other Au-bearing phases (e.g. Au-tellurides) were identified in the paragenesis, thus indicating that the sulphotellurides studied may have precipitated from a hydrothermal fluid that was depleted in precious metals. This is in contrast to the majority of Bi-sulphotelluride enriched mineral systems described in the literature, which usually host significant Au and/or Ag contents.

Numerous Au–Ag–Bi–Te–S-bearing mineral systems have been described elsewhere, and they are commonly interpreted to have precipitated under either high-temperature hydrothermal (e.g., Czamanske & Hall 1975; Ren 1986), or under epithermal conditions (e.g., Oberthür & Weiser 2008). Various phases from the tetradymite group minerals (with unknown phases) together with sulphosalts were described from plenty of localities worldwide (Gu et al. 2001; Cook & Ciobanu 2004; Pieczka et al. 2009; Ciobanu at al. 2010; Cockerton & Tomkins 2012; Voudouris et al. 2013).

Conditions of formation of the Bi–Pb–Sb–S–Te association

The Bi–Pb–Sb–S–Te mineral associations, found in the external host rocks adjacent to the skarn-related orebody, are closely related to previously described skarn-related and breccia-filled types of mineral associations and reveal a similar high-temperature character of formation (Kołodziejczyk et al. 2016a,b). The sulphotelluride mineralization predates Ag mineralization that formed in later stages of ore precipitation at the Stan Terg deposit (Kołodziejczyk et al. 2016a,b).

The sulphotelluride association in the Stan Terg deposit seems to be closely related to cosalite and lillianite, and occurs in most cases with ikunolite and native bismuth as inclusions or as intergrowths with cosalite. The sulphotellurides could have precipitated after galena as a result of introduction of Bi, Sb and Te into the system by hydrothermal fluids, which enabled the formation of Bi-sulphosalts and sulphotellurides.

The lamellar exsolution textures observed in lillianite at Stan Terg, are similar to those described for the Ocna de Fier Fe–Cu skarn deposit, Banat (southwest Romania) by Ciobanu and Cook (2000), and indicate breakdown from the decomposition of high-temperature initially formed crystals. The temperature of initial mineralization may exceed 400 ºC as suggested by Ciobanu & Cook (2000), in accordance with experimental studies in the Cu–Pb–Bi–Ag-bearing systems (Chang et al. 1988). As suggested by Ciobanu & Cook (2000) for the Ocna de Fier, it is believed that intergrowths of Bi-sulphosalts and sulphotellurides at Stan Terg reflect modulated growth processes in a metasomatic environment.

Conclusions

A new occurrence of Bi-sulphotellurides at the Stan Terg hydrothermal system, is associated with galena and Bi- and Sb-sulphosalts.

The Bi-sulphotellurides include joséite-A, joséite-B, and two other phases (phase A and phase B), that could not be assigned to any known mineral due to the lack of structural data. Bi↔Te substitution and admixtrure with submicroscopic PbS and or Bi–Pb sulphotelluride layers, as well as lattice-scale incorporation of Bi–(Pb)-rich modules are considered to explain dispersion of our results along distinct geochemical trends.

Cosalite from the Stan Terg deposit displays high Sb (max. 3.94 apfu), and low Cu and Ag (max. 0.72 Cu+Ag apfu) contents.

Neither the sulphotellurides, nor the accompanying sulphosalts, incorporate abundant Ag in their structures. Gold and silver sulphotellurides have not been found in this association. The hydrothermal fluids could have been either depleted in precious metals, or the physico-chemical conditions of ore formation prevented Au and Ag precipitation at the site of ore deposition.

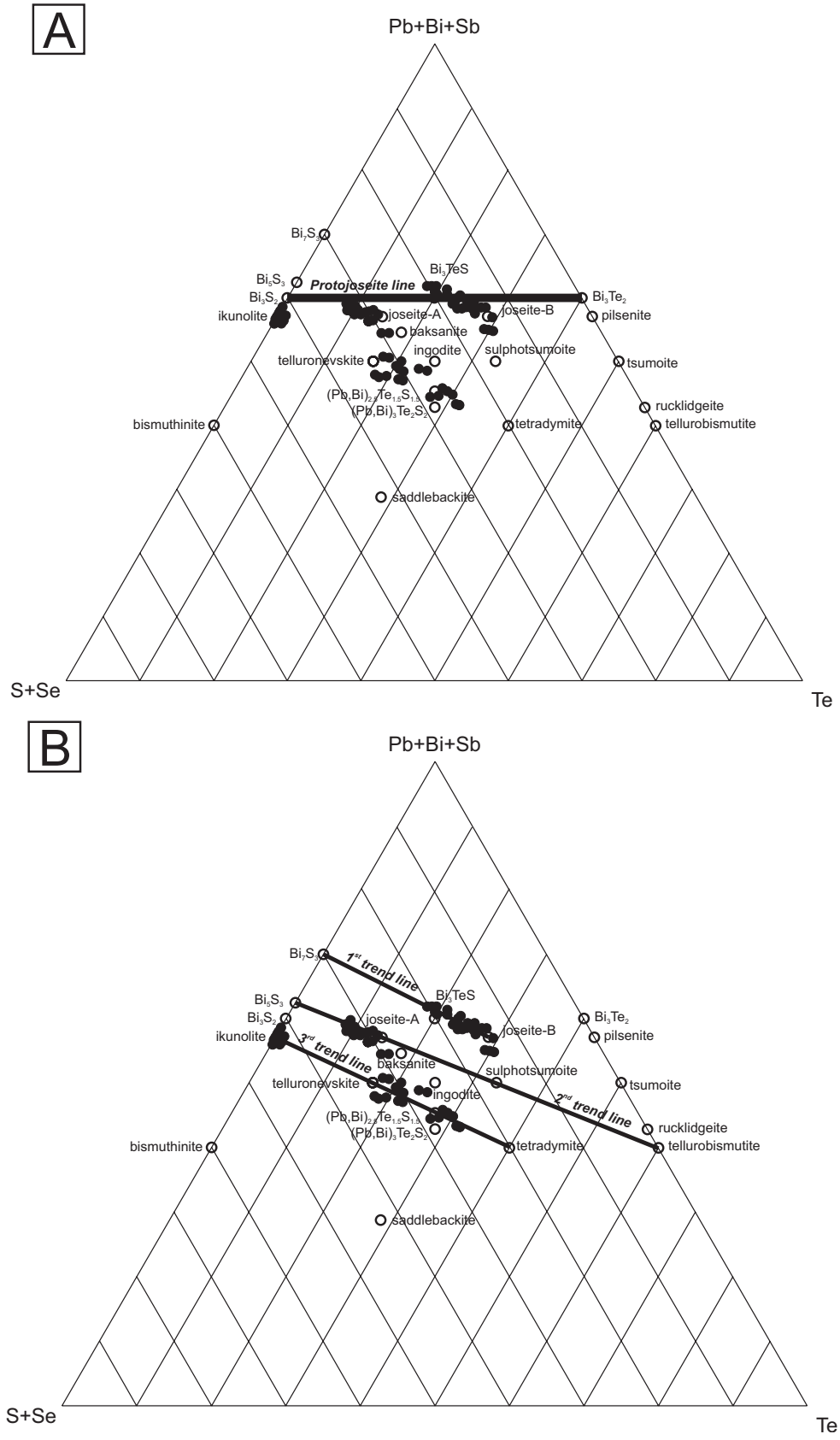

Fig. 9. Ternary plot Bi+Pb+Sb vs S+Se vs Te of Bi-sulphotelluride minerals from the Stan Terg mine. Open circles: minerals ideal end member chemical compositions; solid black symbols: chemical compositions of minerals from the Stan Terg deposit. Protojoseite line is drawn according to general formula $Bi_3(Te,S)_2$ given by Cook et al. (2007a).

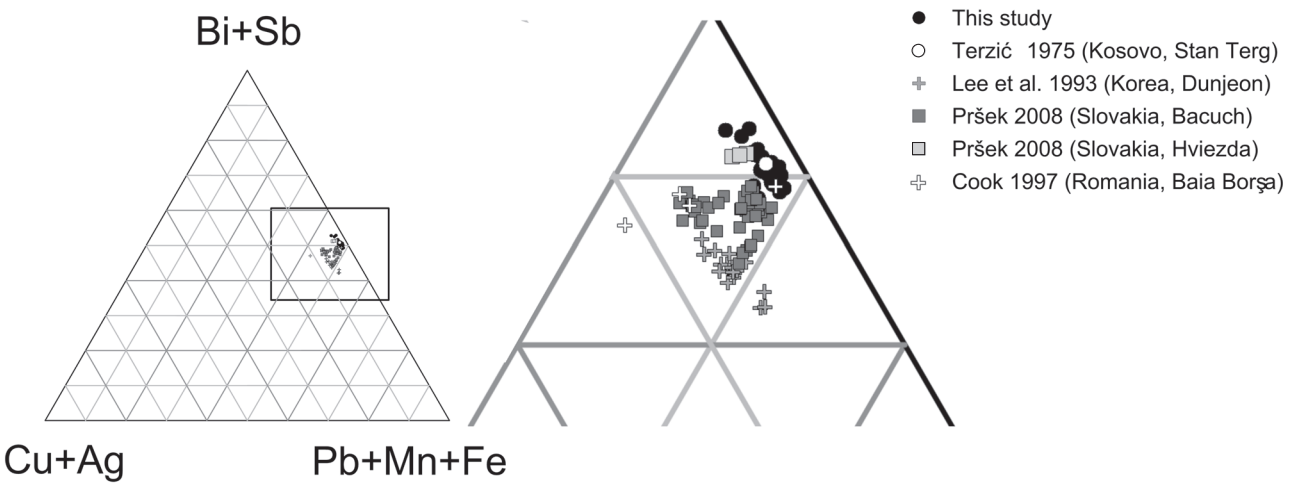

Fig. 10. Ternary plot Cu+Ag vs Bi+Sb vs Pb+Mn+Fe of cosalite — new EPMA data for Stan Terg, described as cosalite in the Stan Terg mine and other Sb-rich cosalite.

Acknowledgements: The research was financed by the AGH University of Science and Technology grants No. 11.11.140.320 and 15.11.140.636. Two anonymous reviewers are greatly acknowledged for their constructive comments that highly improved the earlier version of the manuscript. Associate Editor is especially thanked for the editorial handling of the manuscript.

References

Bowell R.J., Foster R.P. & Stanley C.J. 1990: Telluride mineralization at Ashanti gold mine, Ghana. *Mineral. Mag.* 54, 617–627.

Cepedal A., Martinez-Abad I., Fuertes-Fuente M. & Lima A. 2013: The presence of plumboan ingodite and a rare Bi-Pb telluro-sulfide, Pb3Bi4Te4S5, in the Limarinho Gold deposit, Northern Portugal. *Can. Mineral.* 51, 643–651.

Chang L.L.Y., Wu D. & Knowles C.R. 1988: Phase relations in the system Ag_2S–Cu_2S–PbS–Bi_2S_3. *Econ. Geol.* 83, 405–418.

Ciobanu C.L. & Cook N.J. 2000: Intergrowths of bismuth sulphosalts from the Ocna de Fier Fe-skarn deposit, Banat, Southwest Romania. *Eur. J. Mineral.* 12, 899–917.

Ciobanu C.L., Cook N.J., Pring A., Brugger J., Danyushevsky L.V. & Shimizu M. 2009a: 'Invisible gold' in bismuth chalcogenides. *Geochim.Cosmochim. Acta* 73, 7, 1970–1999.

Ciobanu C.L., Pring A., Cook N.J., Self P., Jefferson D., Dima G. & Melnikov V. 2009b: Chemical-structural modularity in the tetradymite group: a HRTEM study. *Am. Mineral.* 94, 517–534.

Ciobanu C.L., Birch W.D., Cook N.J., Pring A. & Grundler P.V. 2010: Petrogenetic significance of Au–Bi–Te–S associations: The example of Maldon, Central Victorian gold province, Australia. *Lithos* 116, 1–17.

Cockerton A.B.D. & Tomkins A.G. 2012: Insights into the liquid bismuth collector model through analysis of the Bi-Au Stormont skarn prospect, northwest Tasmania. *Econ. Geol.* 107, 667–682.

Cook N.J. 1997: Bismuth and bismuth-antimony sulphosalts from Neogene vein mineralisation, Baia Borşa area, Maramureş, Romania. *Mineral. Mag.* 61, 3, 387–409.

Cook N.J. & Ciobanu C.L. 2004: Bismuth tellurides and sulphosalts from the Larga hydrothermal system, Metaliferi Mts, Romania: paragenesis and genetic significance. *Mineral. Mag.* 68, 2, 301–321.

Cook N.J., Ciobanu C.L., Wagner T. & Stanley C.J. 2007a: Minerals of the system Bi-Te-Se-S related to the tetradymite archetype: Review of classification and compositional variation. *Can. Mineral.* 45, 665–708.

Cook N.J., Ciobanu C.L., Stanley C.J., Paar W. & Sundblad K. 2007b: Compositional data for Bi-Pb tellurosulfides. *Can. Mineral.* 45, 417–435.

Cook N.J., Ciobanu C.L., Spry P.G. & Voudouris P. 2009: Understanding gold–(silver)–telluride–(selenide) mineral deposits. *Episodes* 32, 249–263.

Czamanske G.K. & Hall W.E. 1975: The Ag–Bi–Pb–Sb–S–Se–Te mineralogy of the Darwin lead-silver-zinc deposit, southern California. *Econ. Geol.* 70, 6, 1092–1110.

Dangić A. 1993: Tetriary lead-zinc ore deposits and calco-alcaline magmatism of the serbo-macedonian province: metallogenic and geochemical characteristics, hydrothermal systems and their evolution. *Annales Géologiques de la Péninsule Balkanique*, Belgrade, 57, 1, 257–285.

Féraud J. & Deschamps Y. 2009: French scientific cooperation 2007–2008 on the Trepça lead-zinc-silver mine and the gold potential of Novo Brdo/Artana tailings (Kosovo). *BRGM Report No RP-57204-FR*. 1–92, 13 figs., 4 tabl., 18 photos, 1 appendix.

Féraud J., Maliqi G. & Meha V. 2007: Famous mineral localities: The Trepča mine Stari Trg, Kosovo. *Mineral. Rec.* 38, 267–298.

Forgan C.B. 1950: Ore deposits at the Stan Terg lead-zinc mine International Geological Congress. Report of the eighteenth session Great Britain 1984. Part VII. In: Symposium and proceedings of section F. The Geology, paragenesis and reserves of the ores of lead and zinc, Yugoslavia, 290–307.

Groves D.I. & Hall S.R. 1978: Argentian pentlandite with parkerite, joséite A and the probable Bi-analogue of ullmannite from Mount Windarra, Western Austalia. *Can. Mineral.* 16, 1–7.

Gu X., Watanabe M., Hoshino K. & Shibata Y. 2001: Mineral chemistry and associations of Bi-Te(S,Se) minerals from China. *Neues Jahrb. Mineral. Monatsh.* 7, 289–309.

Hyseni S., Durmishaj B., Fetahaj B., Shala F., Berisha A. & Large D. 2010: Trepça Ore Belt and Stan Terg mine – Geological overview and interpretation. Kosovo (SE Europe). *Geologija* 53, 1, 87–92.

Jambor J.L. 1984: New mineral names. *Am. Mineral.* 69, 1190–1196.

Janković S. 1995: The principal metallogenic features of the Kopaonik District. In: Geology and Metallogeny of the Kopaonik Mt. Symposium. Belgrade, 79–101.

Kołodziejczyk J., Pršek J., Melfos V., Voudouris P.Ch., Maliqi F. & Kozub-Budzyń G. 2015. Bismuth minerals from the Stan Terg deposit (Trepça, Kosovo). *Neues Jahrb. Mineral. Abh.* 192, 3, 317–333.

Kołodziejczyk J., Pršek J., Asllani B. & Maliqi F. 2016a: The paragenesis of silver minerals in the Pb-Zn Stan Terg deposit, Kosovo: an example of precious metal epithermal mineralization. *Geology, Geophysics and Environment* 42, 1, 19–29.

Kołodziejczyk J., Pršek J., Voudouris P., Melfos V. & Asllani B., 2016b: Sn-Bearing Minerals and Associated Sphalerite from Lead-Zinc Deposits, Kosovo: An Electron Microprobe and LA-ICPMS Study. *Minerals* 6, 2, 42.

Lee C.H., Park H.I. & Chang L.L. 1993: Sb-cosalite from Dunjeon gold mine, Taebaeg City, Korea. *Mineral. Mag.* 57, 3, 527–530.

Melnikov V., Jeleň S., Bondarenko S., Balintová T., Ozdín D. & Grinchenko A. 2009: Comparative Study of Bi-Te-Se-S Mineralizations in Slovak Republic and Transcarpathian Region of Ukraine. *Mineralogicheskiy Zhurnal* 31, 4, 38–48.

Moëlo Y., Makovicky E., Mozgova N.N., Jambor J.L., Cook N.J., Pring A., Paar W., Nickel E.H., Graeser G., Karup-Møller S., Balić-Žunić T., Mumme W.G., Vurro V., Topa D., Bindi L., Bente K. & Shimizu M. 2008: Sulfosalt systematics: a review. Report of the Sulfosalt Sub-committee of the IMA Commission on Ore Mineralogy. *Eur. J. Mineral.* 20, 7–46.

Oberthür T. & Weiser T.W. 2008: Gold-bismuth-telluride-sulphide assemblages at the Viceroy Mine, Harare-Bindura-Shamva greenstone belt, Zimbabwe. *Mineral. Mag.* 72, 4, 953–970.

Pieczka A., Gołębiowska B. & Parafiniuk J. 2009: Conditions of formation of polymetallic mineralization in the eastern envelope of the Karkonosze granite: the case of Rędziny, southwestern Poland. *Can. Mineral.* 47, 4, 765–786.

Plotinskaya O.Y., Damian F., Prokofiev V.Y., Kovalenker V.A. & Damian G. 2009: Tellurides occurrences in the Baia Mare region, Romania. *Carpathian Journal of Earth and Environmental Sciences* 4, 2, 89–100.

Pršek J. 2004: Chemical composition and crystalochemistry of sulphosalts from sulphide mineralization in Western Carpathians. *Unpublished PhD thesis*, *Comenius University*, Bratislava, Slovakia, 1–135 (in Slovak).

Pršek J. 2008: Chemical composition and crystalochemistry of Bi sulphosalts from the hydrothermal mineralizations of Western Carpatians basement. *State Geological Survey of Slovak Republic press*, 1–108 (in Slovak).

Pršek J. & Chovan M. 2001: Hydrothermal Carbonate and Sulphide Mineralization in the Late Paleozoic Phyllites (Bacúch, Low Tatras Mts.). *Geolines* 13, 27–34.

Pršek J. & Peterec D. 2008: Bi-Se-Te mineralization from Úhorná (Spišsko Gemerské Rudohorie Mts., Słovakia): A preliminary report. *Mineralogia* 39, 3–4, 87–103.

Pršek J., Ozdín D. & Sejkora J. 2008: Eclarite and associated Bi sulfosalts from the Brezno-Hviezda occurrence (Nízke Tatry Mts, Slovak Republic). *Neues Jahrb. Mineral. Abh.* 185, 2, 117–130.

Ren Y.C. 1986: Tellurobismuthinides from Pangushan, China. *Chinese Journal of Geochemistry* 5, 3, 277–279.

Schumacher F. 1950: Trepča deposit and its vicinity. *Publishing House of Council for Energy and Extractive Industry of the FPRY*, Belgrad, 1–65 (in German).

Strmić Palinkaš S., Palinkaš L.A., Renac C., Spangenberg J.E., Lüders V., Molnar M. & Maliqi G. 2013: Metallogenic Model of the Trepča Pb-Zn-Ag Skarn Deposit, Kosovo: Evidence from Fluid Inclusions, Rare Earth Elements, and Stable Isotope Data. *Econ. Geol.* 108, 135–162.

Terzić S.B., Sommerauer J. & Harnik A.B. 1974: Macroscopic cosalite crystals from the Pb-Zn Ore Deposit Trepča (Yugoslavia). *Schweiz. Mineral. Petrogr. Mitt.* 54, 209–211.

Terzić S.B., Sommerauer J. & Harnik A.B. 1975: Needle galena and cosalite from the Stan Terg–Trepča. *Bulletin du Museum d'histoire naturelle*, Belgrade, Serie A, Livre 30, 5–12 (in Serbo-Croatian).

Topa D. & Makovicky E. 2010; The crystal chemistry of cosalite based on new electron-microprobe data and single-crystal determinations of the structure. *Can. Mineral.* 48, 5, 1081–1107.

Vikentyev I.V. 2006: Precious metal and telluride mineralogy of large volcanic-hosted massive sulfide deposits in the Urals. *Mineral. Petrol.* 87, 3–4, 305–326.

Voudouris P., Spry P.G., Mavrogonatos C., Sakellaris G.A., Bristol S.K., Melfos V. & Fornadel A. 2013: Bismuthinite derivatives, lillianite homologues, and bismuth sulfotellurides as indicators of gold mineralization at the Stanos shear-zone related deposit, Chalkidiki, northern Greece. *Can. Mineral.* 51, 119–142.

Zav'yalov Y.N. & Begizov V.D. 1983: New data on the constitution and nomenclature of the sulfotellurides of bismuth of the joseite group. *Zap. Vses. Mineral. Obshchest*. 112, 589–601 (in Russian).